Journal of Physiology (1998), **507.1**, *pp.*93–103

Facilitation by the β_{2a} subunit of pore openings in cardiac Ca^{2+} channels

James Costantin*, Francesca Noceti*, Ning Qin*, the late Xiangyang Wei, Lutz Birnbaumer*† and Enrico Stefani*‡§

*Departments of *Anesthesiology, ‡Physiology and †Biological Chemistry, UCLA School of Medicine, UCLA, Los Angeles, CA 90095, USA and §Conicet, Buenos Aires, Argentina*

(Received 3 July 1997; accepted after revision 16 October 1997)

1. Single channel recordings were performed on the cardiac calcium channel (α_{1C}) in order to study the effect of coexpression of the accessory β_{2a} subunit. On-cell patch clamp recordings were performed after expression of these channels in *Xenopus* oocytes.

2. The α_{1C} subunit, when expressed alone, had similar single channel properties to native cardiac channels. Slow transitions between low and high open probability (P_o) gating modes were found as well as fast gating transitions between the open and closed states.

3. Coexpression of the β_{2a} subunit caused changes in the fast gating during high P_o mode. In this mode, open time distributions reveal at least three open states and the β_{2a} subunit favours the occupancy of the longest, 10–15 ms open state. No effect of the β_{2a} subunit was found when the channel was gating in the low P_o mode.

4. Slow gating transitions were also affected by the β_{2a} subunit. The high P_o mode was maintained for the duration of the depolarizing pulse in the presence of the β_{2a} subunit; while the α_{1C} channel when expressed alone, frequently switched into and out of the high P_o mode during the course of a sweep.

5. The β_{2a} subunit also affected mode switching that occurred between sweeps. Runs analysis revealed that the α_{1C} subunit has a tendency toward non-random mode switching. The β_{2a} subunit increased this tendency. A χ^2 analysis of contingency tables indicated that the β_{2a} subunit caused the α_{1C} channel to gain 'intrinsic memory', meaning that the mode of a given sweep can be non-independent of the mode of the previous sweep.

6. We conclude that the β_{2a} subunit causes changes to the α_{1C} channel in both its fast and slow gating behaviour. The β_{2a} subunit alters fast gating by facilitating movement of the channel into an existing open state. Additionally, the β_{2a} subunit decreases the slow switching between low and high P_o modes.

High voltage activated cardiac calcium channels are multimeric proteins that respond to a depolarizing voltage pulse by opening with complex single channel gating behaviour (Pietrobon & Hess, 1990; Delcour & Tsien, 1993; Rittenhouse & Hess, 1994). The channel consists of a transmembrane α_1 subunit that contains the voltage sensor and the ion conducting pore, as well as several accessory subunits β, γ and α_2/δ (Perez-Reyes *et al.* 1989; Catterall, 1991; Hofmann, Biel & Flockerzi, 1994). The function of the accessory subunits has been extensively studied at the macroscopic current level. The β_{2a} subunit increased the magnitude and the speed of activation of α_{1C} macroscopic ionic currents (Lacerda *et al.* 1991; Wei, Perez-Reyes, Lacerda, Schuster, Brown & Birnbaumer, 1991; Singer, Biel, Lotan, Flockerzi, Hofmann & Dascal, 1991; Varadi, Lory, Schultz, Varadi & Schwartz, 1991; Williams *et al.* 1992; Lory, Varadi, Slish, Varadi & Schwartz, 1993; Olcese *et al.* 1994; Pérez-García, Kamp & Marban, 1995). This current potentiation occurred without significant changes in the movement of the voltage sensor, recorded as gating currents (Neely, Wei, Olcese, Birnbaumer & Stefani, 1993). These studies indicated that the β_{2a} subunit facilitated pore opening by improving the coupling between the movement of the voltage sensor and the opening of the channel pore.

Voltage-gated ion channels exhibit fast gating transitions between open and closed states, as well as slow transitions

We dedicate this work to the memory of Xiangyang Wei who recently passed away.

between different modes that have distinct gating behaviour (Moczydlowski & Latorre, 1983; Bean, 1989). In native cardiac Ca^{2+} channels, individual sweeps have been grouped into three modes of gating: (a) null or silent traces with no channel activity; (b) mode 1, low probability of opening (low P_o) traces with infrequent brief openings, and (c) mode 2, medium to high P_o traces with openings clustered forming bursts of activity (Reuter, Stevens, Tsien & Yellen, 1982; Hess, Lansman & Tsien, 1984; Bean, 1990). Native cardiac Ca^{2+} channels can remain in a single mode during sequential sweeps; changes between these three modes of activity are referred to as slow gating transitions. The dihydropyridine agonist Bay K 8644 has been shown to enhance single channel calcium current by increasing the single channel open probability through an increase in the likelihood of mode 2 gating (Hess *et al.* 1984; reviewed by McDonald, Pelzer, Trautwein & Pelzer, 1994). In this study, we investigated whether the regulatory β_{2a} subunit can modify the single channel gating properties of the cardiac α_{1C} subunit expressed in *Xenopus* oocytes in the presence of 10 μM Bay K 8644. The β_{2a} subunit affects fast gating transitions by favouring pore opening and facilitating the open state during high P_o gating; slow gating transitions are affected by a stabilization of a given gating mode, without a change in the proportion of a given mode.

METHODS

Molecular biology and oocyte preparation

The cRNAs were prepared from two plasmids bearing the α-splice variant of the type C or cardiac α_1 ($\alpha_{1C\text{-}a}$) formerly also CaCh2a, and the type 2a cardiac β_{2a} subunit. The α_{1C} cDNA was digested with Hind III as previously described (Wei *et al.* 1991) and β_{2a} cDNA with Not I (Perez-Reyes *et al.* 1992). Linearized plasmids (0·5 μg) were transcribed at 37 °C in a volume of 25 μl containing 40 mM Tris–HCl (pH 7·2), 6 mM $MgCl_2$, 10 mM dithiothreitol, 4 mM spermidine, 0·4 mM each of adenosine triphosphate, guanosine triphosphate, cytosine triphosphate and uridine trisphosphate, 1 mM 7-methyl guanosonine (5′) triphosphate (5′) guanosine and 10 units of T7 RNA polymerase (Boehringer–Mannheim). The cRNA products were extracted with phenol–chloroform, recovered by precipitation with ethanol and suspended in double-distilled water to a final concentration of 0·2 μg μl^{-1} of each species, 50 nl were injected per oocyte.

Xenopus frogs were anaesthetized by immersion in water containing 0·15% tricane methanesulphonate (Sigma) for at least 20 min until fully immobile. The ovaries were surgically removed under sterile conditions by abdominal incision. The animals were then killed by decapitation. Animal protocols were performed with the approval of the Institutional Animal Care Committee of the University of California, Los Angeles. Oocytes were maintained at 19·5 °C in modified Barth's solution containing 90 mM NaCl, 2 mM KCl, 2 mM $CaCl_2$, 2 mM $MgCl_2$, 10 mM Hepes, 50 μg ml^{-1} gentamicin, adjusted to pH 7·2 with NaOH.

Channel recording and data analysis

Recordings were performed 4–12 days following cRNA injection. Single channel activity was recorded with an EPC-7 patch clamp amplifier (List Electronic) from cell-attached patches of *Xenopus* oocyte membrane after removing the vitelline layer. Recording pipettes had tip diameters of 2–6 μm with a final resistance of 0·5–4 MΩ. Stray capacitance was reduced by coating the shank of the pipettes with a mixture of Parafilm and light mineral oil. The pipette solution contained 75 mM $Ba(CH_3SO_3)_2$, 5 mM $BaCl_2$, 10 μM (−)-Bay K 8644 and 10 mM Hepes, titrated to pH 7·0. The bath saline was 110 mM KCH_3SO_3 with 10 mM Hepes titrated to pH 7·0. We used a high (−)-Bay K 8644 concentration, about 200 times higher than its K_d, to minimize any potential effect of the β_{2a} subunit on the binding of (−)-Bay K 8644 to the channel. The data presented were collected from one channel in a patch for any given experiment. Patch potentials were maintained at −50 mV and 200 ms pulses to 15 mV were delivered at 1 Hz. Analysis was performed on seven α_{1C} and eight $\alpha_{1C}+\beta_{2a}$ patches in which we succeeded in recording up to 1000 sweeps. Data were digitized at 50 or 100 μs (point)$^{-1}$ after low-pass filtering at 2 kHz. Single channel records were corrected off-line for linear leak and capacity currents using customized software. Open and closed transitions were detected by the half amplitude threshold criterion using TRANSIT software (VanDongen, 1996). Open and closed time histograms were fitted to multiple exponential functions using the maximum likelihood method (Sigworth & Sine, 1987) and the adequacy of the fit with different numbers of distributions was statistically evaluated, and accepted when $P < 0{\cdot}01$.

Separation of low and high P_o sweeps

Categorization of sweeps was achieved by defining null sweeps as those containing no channel activity, low open probability (low P_o) sweeps were defined as those that exhibited channel activity with an open probability of $P_o \leqslant 0{\cdot}3$, and high P_o sweeps were defined as those that exhibited channel activity with a $P_o > 0{\cdot}3$.

Runs analysis and χ^2 contingency table analysis

Each sweep was categorized into null, low P_o or high P_o mode to perform runs and contingency analysis. Runs analysis evaluates whether the clustering of sweeps with the same mode (i.e. a run) represents a deviation from randomness. This deviation can occur in two ways: (a) the number of runs can be smaller than would randomly occur, in which case the distribution is 'contagious', or (b) the number of runs can be larger than would randomly occur, in which case the distribution is 'uniform'. In our case, the number of runs was always smaller than would randomly occur, thus we tested our data for 'contagiousness'. To do this, we performed one-tailed tests on the statistic Z (the standard random variable) in the case of three nominal categories. Z should a normal deviate for a large number of runs ($n > 30$, Brownlee, 1965; Zar, 1974), and we formulate the null hypothesis in these terms: 'the distribution of Z is non-contagious'. Values of Z are compared to tabulated critical values. The distribution is contagious when $Z \geqslant Z_{\text{critical}}$ and $u \leqslant \mu_u$, where u is the experimental number of runs and μ_u is the mean of the distribution, with standard deviation σ_u. The distribution would be uniform if $Z \geqslant Z_{\text{critical}}$ and $u \geqslant \mu_u$.

Another approach to the clustering of sweeps with the same mode is the χ^2 analysis of contingency tables. Contingency tables (2 × 2) of elements were constructed. The null hypothesis in this case is that the row frequencies (mode during the second sweep) are independent of the column frequencies (mode during the first sweep). In other words, the null hypothesis states that the process has no intrinsic memory and the occurrence of a given mode sweep is independent of the mode of the channel during the previous sweep.

RESULTS

Low and high P_o gating behaviour is present in the α_{1C} subunit

The single channel traces in Fig. 1 are representative of the fast and slow gating behaviour present in the α_{1C} and $\alpha_{1C}+\beta_{2a}$ channels. Channel openings are downward deflections. Ensemble averages (EA) of single channel experiments are shown below the single channel records. Macroscopic patch recordings (MP) from a different oocyte, using the same recording solutions, are superimposed on the ensemble averages for both the α_{1C} and the $\alpha_{1C}+\beta_{2a}$ channel. The close agreement in the time course of the macroscopic currents and the ensemble averages are evidence that the single channel recordings are representative samples. These channels have fast gating transitions between the open and closed states as well as bursts of openings that are closely spaced and that occur during the time interval of a sweep (200 ms). In addition to this fast gating behaviour, a slow gating process can be observed that switches the channel between low and high P_o modes. In both α_{1C} (Fig. 1*A*) and $\alpha_{1C}+\beta_{2a}$ (Fig. 1*B* and *C*), we found null traces, traces with brief openings close to the pulse onset which became infrequent toward the end of the pulse (low P_o) and traces with bursts of channel openings that can occur throughout the duration of the trace (high P_o). Thus, as previously described for native Ca^{2+} channels (Hess *et al.* 1984), expressed Ca^{2+} channels can gate in low and high P_o modes. Furthermore, these data indicate that the α_{1C} subunit, when expressed alone, encodes these modes of gating. The examination of the traces in Fig. 1*A*, *B* and *C* suggests that coexpression of the β subunit modified both fast and slow gating behaviours. The β_{2a} subunit affected the fast gating

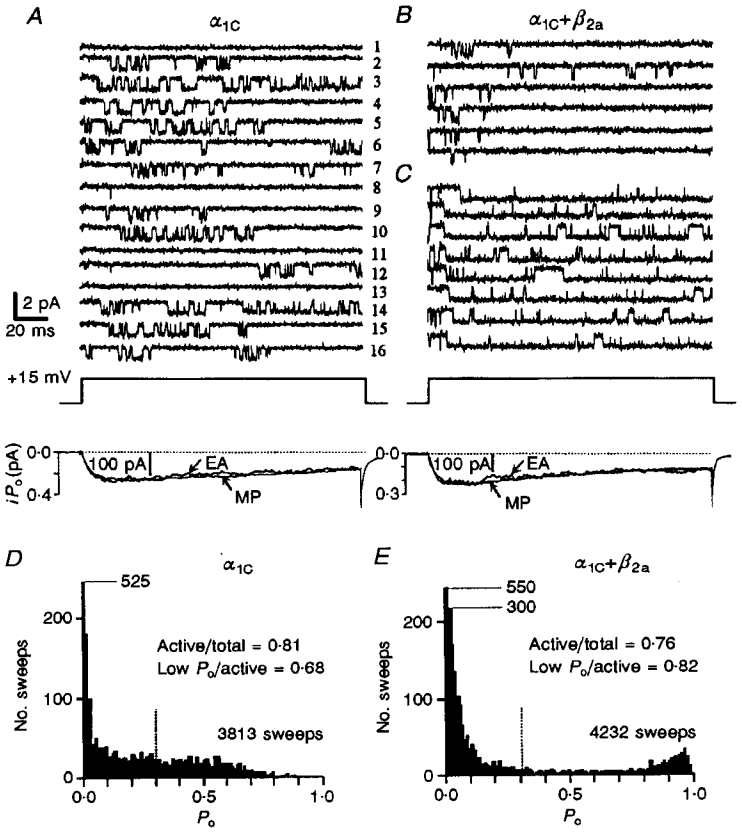

Figure 1. Effect of the β_{2a} subunit on single α_{1C} channels

Coexpression of the β_{2a} subunit affects both fast and slow gating in α_{1C}. Single channel currents through the pore-forming subunit (α_{1C}) of the cardiac Ca^{2+} channel expressed with or without the β_{2a} subunit in oocytes in the presence of 10 μM Bay K 8644. Consecutive sweeps, pulses to +15 mV from a holding potential of −50 mV: α_{1C} channel expressed alone (*A*); $\alpha_{1C}+\beta_{2a}$ low P_o (*B*) and high P_o (*C*) traces. Corresponding ensemble averages (EA) and macroscopic patch currents (MP) from another oocyte are shown below the single channel records. *D*, P_o frequency histogram from seven patches expressing the α_{1C} subunit alone. *E*, P_o frequency histogram from eight patches co-expressing the $\alpha_{1C}+\beta_{2a}$ subunit. Bin width is 0·01. Vertical dashed line indicates $P_o = 0·3$.

Table 1. Effect of coexpression of β_{2a} subunit on open times

	τ_1 (ms)	A_1 (pA)	τ_2 (ms)	A_2 (pA)	τ_3 (ms)	A_3 (pA)	Mean open time (ms)
α_{1C}							
All sweeps	0·76 ± 0·16	0·34 ± 0·15	2·55 ± 0·45	0·63 ± 0·26	8·82 ± 1·98	0·04 ± 0·07	2·02 ± 0·24
High P_o	1·10 ± 0·18	0·44 ± 0·13	2·95 ± 0·23	0·61 ± 0·09	8·49 ± 0·89	0·06 ± 0·02	2·68 ± 0·30
Low P_o	1·15 ± 0·23	0·77 ± 0·11	2·91 ± 0·18	0·40 ± 0·11	—	—	1·66 ± 0·13
$\alpha_{1C}+\beta_{2a}$							
All sweeps	0·56 ± 0·06 (0·31)	0·34 ± 0·04 (1·00)	2·26 ± 0·42 (0·62)	0·49 ± 0·10 (0·26)	14·46 ± 2·74 (0·05)	0·31 ± 0·06 (0·008)	5·55 ± 1·35 (0·04)
High P_o	—	—	2·53 ± 0·55 (0·37)	0·47 ± 0·09 (0·19)	13·34 ± 1·17 (0·01)	0·61 ± 0·10 (0·001)*	10·99 ± 1·46 (0·001)*
Low P_o	1·32 ± 0·16 (0·74)	0·91 ± 0·04 (0·28)	5·10 ± 0·72 (0·04)	0·09 ± 0·04 (0·13)	—	—	2·34 ± 0·12 (0·35)

Values are means ± S.E.M. Seven and eight experiments for α_{1C} and $\alpha_{1C}+\beta_{2a}$, respectively. Numbers in parentheses are Student's t test-derived probabilities with two independent samples and two-tailed distribution. * Statistically significant.

properties by increasing burst duration and the proportion of long openings during a high P_o burst. The β_{2a} subunit affected the slow gating properties by stabilizing a given gating mode during consecutive sweeps.

Long openings during bursts of activity are favoured by coexpression of the β subunit

We defined the three modes of gating for further analysis as follows: null sweeps were the sweeps with no channel activity; low P_o sweeps were those with a $P_o \leqslant 0{\cdot}3$, and high P_o sweeps were those with a $P_o > 0{\cdot}3$. Examples of these modes can be seen in the single channel traces of Fig. 1, for the α_{1C} channel, null (sweeps 1, 11 and 13), low P_o (sweeps 2, 7, 8 and 9) and high P_o (sweeps 3, 5, 10, 14 and 15). $\alpha_{1C}+\beta_{2a}$ openings are shown in Fig. 1*B* (low P_o), and Fig. 1*C* (high P_o). Low P_o sweeps are indistinguishable between α_{1C} and $\alpha_{1C}+\beta_{2a}$ channels. High P_o openings are, however, quite distinct when comparing α_{1C} and $\alpha_{1C}+\beta_{2a}$ channels (e.g. compare sweep 10 in Fig. 1*A* with any sweep in Fig. 1*C*). High P_o can be identified for both clones by clusters of openings separated by closings generating bursts of channel activity. The $\alpha_{1C}+\beta_{2a}$ bursting pattern is different in that the openings during the burst, and the duration of the bursts, are longer (Fig. 1*C*), and consequently the closures during a high P_o burst are shorter. These differences were quantitatively investigated by the construction and analysis of open and closed dwell time histograms.

Coexpression of the β_{2a} subunit stabilizes bursting activity during high P_o

Coexpression of the β_{2a} subunit also caused changes in slow gating processes. In the absence of the β_{2a} subunit, the channel frequently switched into, and out of, high P_o during a sweep (Fig. 1*A*), whereas in the presence of the β_{2a} subunit, a sweep that began in a particular mode tended to remain in that mode for the duration of the sweep (Fig. 1*B* and *C*). These gating properties are reflected in the P_o frequency histograms compiled from all of the experiments for the α_{1C} and the $\alpha_{1C}+\beta_{2a}$ channels (Fig. 1*D* and *E*). In the presence of the β_{2a} subunit, the histogram closely resembled that seen for native channels (Hess *et al.* 1984): there is a peak at very low P_o, and a peak at very high P_o, with relatively few sweeps exhibiting intermediate values of P_o (between 0·3 and 0·6). This form of the histogram indicated that most of the sweeps were clearly separated as low or high P_o. In the absence of the β_{2a} subunit (Fig. 1*D*), the histogram had a similar peak at very low P_o, but it did not have a distinct peak at higher P_o, and it had a shallow distribution at intermediate P_o values. This shallow P_o distribution in conjunction with the visual examination of raw sweeps suggested that the intermediate P_o sweeps, in the absence of the β_{2a} subunit, were due to bursts of high P_o gating that were not maintained for the entire duration of the sweep (see sweeps 5, 10, 14 and 15 in Fig. 1*A*).

Coexpression of the β_{2a} subunit does not change the proportion between the different gating modes

To investigate whether the β_{2a} subunit affected the proportion of the different gating modes, we compared the proportion of null, low P_o and high P_o sweeps for α_{1C} *versus* $\alpha_{1C}+\beta_{2a}$. The gating modes were categorized as described above. The insets in Fig. 1*D* and *E* show that the β_{2a} subunit caused no significant change in the overall proportion of null, low P_o or high P_o sweeps. In all of the experiments combined for α_{1C} and $\alpha_{1C}+\beta_{2a}$, respectively, the fraction of null sweeps was 0·19 ± 0·05 and 0·24 ± 0·15, the fraction of low P_o sweeps was 0·55 ± 0·07 and 0·62 ± 0·02, and, the fraction of high P_o sweeps was 0·25 ± 0·06 and 0·13 ± 0·13.

Effect of β_{2a} subunit coexpression on open dwell times

Changes to fast gating kinetics caused by β_{2a} subunit coexpression were studied by measuring the distributions of

open and closed dwell times. In all cases, open times could be fitted to the sum of three distributions with a fast τ near 1 ms, an intermediate τ near 2–4 ms and a slow τ near 10–15 ms. The histograms in Figs 2 and 3 correspond to all events combined for α_{1C} alone (54 392 events from 7 patches, upper panel) and for $\alpha_{1C}+\beta_{2a}$ (29 135 events from 8 patches, lower panel). Table 1 summarizes the means ± S.E.M. for the different open dwell time components in α_{1C} and $\alpha_{1C}+\beta_{2a}$. The number in parentheses is the statistical significance for each value, comparing α_{1C} and $\alpha_{1C}+\beta_{2a}$. The histograms and table show that the open times, with and without β_{2a}, could be fitted by similar time constant values but with differing weights. The main action of the β_{2a} subunit on the fast gating kinetics was to increase the fraction of the third open time distribution from 0·04 to 0·10 (Fig. 2, A_{o3} values). The fact that the β_{2a} subunit did not significantly change the time constant values of the open time distributions, suggests that coexpression of the β_{2a} subunit did not create a new open state, but it favoured the frequency of occupancy of an existing long open state.

To investigate whether low or high P_o modes were preferentially altered by the β_{2a} subunit, we constructed separate open dwell time histograms from sweeps containing only low (Fig. 3*A* and *C*) or high P_o (Fig. 3*E* and *G*) sweeps. The sweeps were categorized into high and low P_o separated at $P_o = 0·3$ as described in Methods. These histograms were simultaneously fitted with three time constants in each mode, with and without the β_{2a} subunit. The data show that the β_{2a} subunit did not greatly modify the open times during low P_o, while it increased the mean open time during high P_o gating. This large increase in the mean open time in high P_o results from a larger fraction of long openings (τ_{o3}) which increased from 0·04 in α_{1C} to 0·59 in $\alpha_{1C}+\beta$ (Fig. 3*E* and *G*). The coexpression of the β_{2a} subunit also increased the burst duration during high P_o (Fig. 1). Bursts were identified as gating activity separated by closed time longer than 8·5 ms, which was derived from the closed dwell time histograms (Fig. 4). The mean burst duration increased from 35 ms in α_{1C} alone to 44 ms in $\alpha_{1C}+\beta_{2a}$ channels, while the average number of openings per burst did not significantly change (9·0 events in α_{1C} and 7·4 events in $\alpha_{1C}+\beta_{2a}$). In summary, coexpression of the β_{2a} subunit favoured pore opening during high P_o by increasing the frequency of long openings during bursts of activity and increasing the mean duration of the bursts.

Ca^{2+} channel inactivation follows only brief openings in low P_o

Ensemble average currents are to the right of each corresponding open time histogram in Fig. 3. The average current was maintained during the pulse length in high P_o

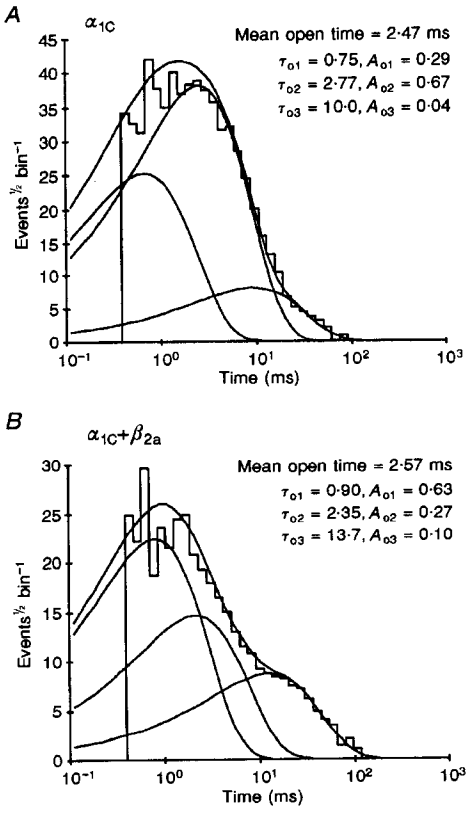

Figure 2. Open dwell time histograms

Coexpression of the β_{2a} subunit increases the proportion of long openings. Fits of the open dwell time histograms to exponential distributions using the maximum likelihood method. α_{1C} (*A*) and $\alpha_{1C}+\beta_{2a}$ (*B*). The histograms are obtained from all data combined together, bin width is 0·07. In both panels, the continuous lines are the fits to the individual components and to the total histogram. Values of the time constants (τ_{o1}, τ_{o2} and τ_{o3}, in ms) and of the respective relative amplitudes (A_{o1}, A_{o2} and A_{o3}) are given for both α_{1C} and $\alpha_{1C}+\beta_{2a}$. Recordings were performed in the presence of 10 μM Bay K 8644.

sweeps, while in low P_o sweeps the currents inactivated. This was seen at the single channel level as brief openings clustered in the first half of the sweep during low P_o, while during high P_o the openings occurred throughout the duration of the sweep. This finding suggests that the inactivated state is reached from the low P_o mode of gating.

Effect of β subunit coexpression on closed times

The results of the analysis for the closed dwell times are shown in Figs 4 and 5. Figure 4 illustrates the closed dwell time histograms for α_{1C} and $\alpha_{1C}+\beta_{2a}$ channels for all traces, while in Fig. 5 low and high P_o traces were separated. We could not detect any effect of the coexpression of the β_{2a}

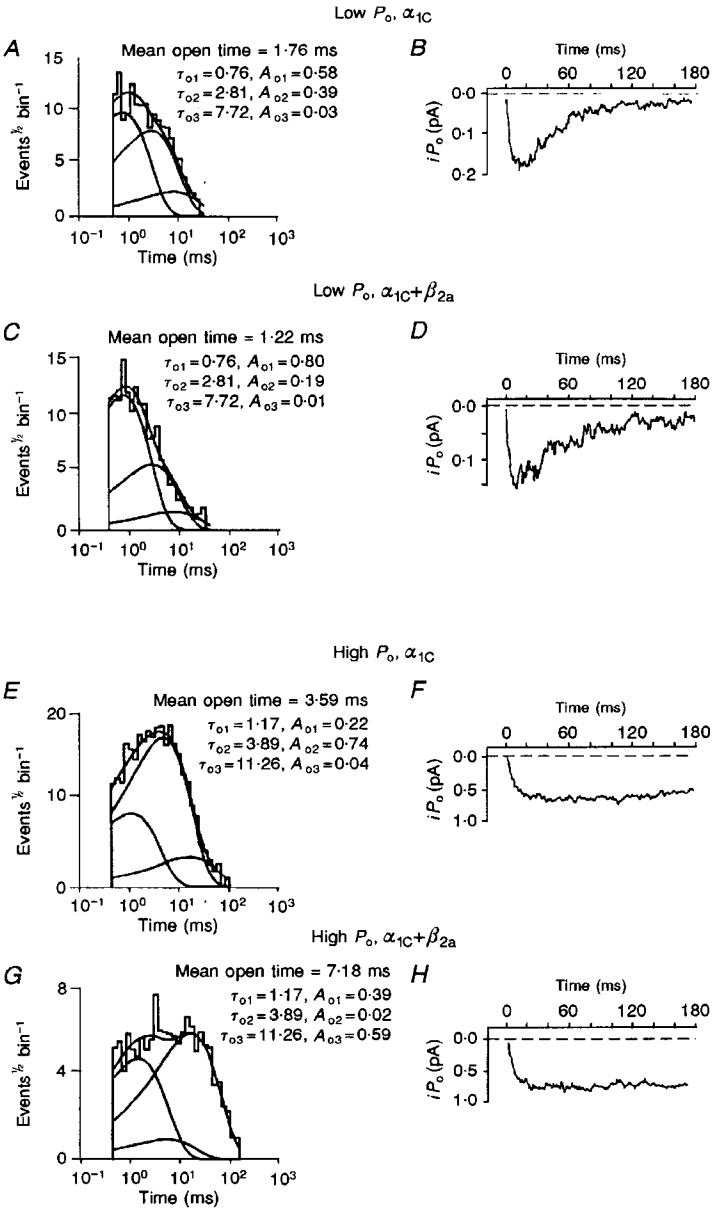

Figure 3. Open dwell time histograms for low and high P_o

The β_{2a} subunit favours the occurrence of long openings only in high P_o. Simultaneous fits of open dwell time histograms, with ($\alpha_{1C}+\beta_{2a}$, *C* and *G*) and without (α_{1C}, *A* and *E*) the β_{2a} subunit, after separation of high P_o (*E* and *G*) and low P_o (*A* and *C*) sweeps. The histograms have been fitted in pairs, α_{1C} and $\alpha_{1C}+\beta_{2a}$ in each mode, forcing the time constants to the same values for the pair and allowing the respective amplitudes to change for each histogram, bin width is 0·07. Ensemble averages are shown to the right of corresponding histograms (*B*, *D*, *F* and *H*). Recordings were performed in the presence of 10 μM Bay K 8644.

Table 2. Effect of coexpression of β_{2a} subunit on closed times

	τ_1 (ms)	A_1 (pA)	τ_2 (ms)	A_2 (pA)	τ_3 (ms)	A_3 (pA)	Mean closed time (ms)
α_{1C}							
All sweeps	0·74 ± 0·12	0·66 ± 0·07	4·37 ± 0·51	0·24 ± 0·03	33·73 ± 6·70	0·10 ± 0·05	4·06 ± 0·78
High P_o	0·64 ± 0·10	0·56 ± 0·04	2·74 ± 0·43	0·37 ± 0·07	12·50 ± 1·87	0·07 ± 0·07	2·14 ± 0·96
Low P_o	0·79 ± 0·12	0·59 ± 0·07	6·77 ± 0·66	0·27 ± 0·02	41·30 ± 7·86	0·14 ± 0·06	7·17 ± 2·01
$\alpha_{1C}+\beta_{2a}$							
All sweeps	0·56 ± 0·03 (0·18)	0·54 ± 0·06 (0·19)	6·57 ± 0·71 (0·03)	0·28 ± 0·34 (0·32)	49·90 ± 7·80 (0·12)	0·18 ± 0·05 (0·30)	9·71 ± 1·82 (0·02)
High P_o	0·47 ± 0·05 (0·15)	0·77 ± 0·03 (0·001)*	3·80 ± 0·80 (0·20)	0·20 ± 0·03 (0·05)	17·15 ± 3·94 (0·23)	0·05 ± 0·01 (0·70)	1·65 ± 0·24 (0·67)
Low P_o	0·81 ± 0·13 (0·94)	0·43 ± 0·05 (0·06)	7·24 ± 0·68 (0·08)	0·35 ± 0·04 (0·05)	38·18 ± 5·16 (0·95)	0·22 ± 0·06 (0·26)	10·71 ± 1·95 (0·12)

Values are means ± S.E.M. Seven and eight experiments for α_{1C} and $\alpha_{1C}+\beta_{2a}$, respectively. Numbers in parentheses are Student's t test-derived probabilities with two independent samples and two-tailed distribution. * Statistically significant.

subunit on the overall closed time distribution in the histograms containing all modes. To investigate possible actions of the β_{2a} subunit further, we performed a separate analysis for low and high P_o sweeps. In low P_o, the data are indistinguishable, but in high P_o coexpression of the β_{2a} subunit significantly increased (see Table 2) the proportion of the briefer closed times, which resulted in a modest reduction of the mean closed times. The faster exit from the closed state is in agreement with the higher frequency of long openings with the β_{2a} subunit. In summary, by

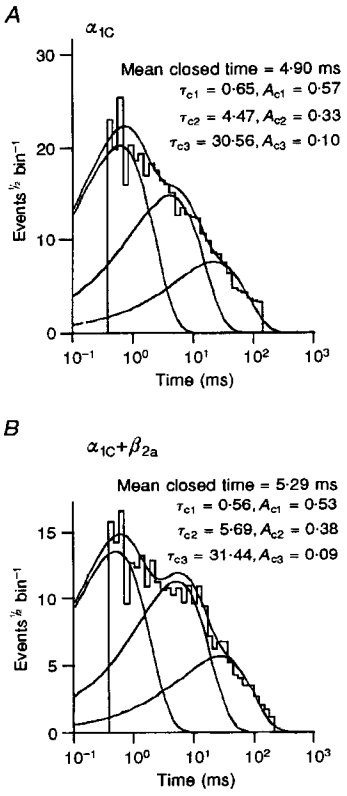

Figure 4. Closed dwell time histograms

Changes in the overall closed time distribution in the presence of the β_{2a} subunit were not detected when using all mode sweeps. Closed time histograms for α_{1C} (*A*) and $\alpha_{1C}+\beta_{2a}$ (*B*), bin width is 0·07. As in Fig. 2, all events have been combined and fits to the individual components are shown together with the fits to the total histograms. Bay K 8644 (10 μM) is present.

increasing the rates from the closed to the open states the β_{2a} subunit favours channel opening without changing the conformation of the open channels.

Effect of β_{2a} subunit coexpression on mode switching between consecutive sweeps

We performed runs analysis (Plummer & Hess, 1991) to determine whether the β_{2a} subunit caused the channel to remain in a particular gating mode for a longer series of consecutive sweeps (i.e. a run). The three population runs analysis compared runs of sweeps that had been classified into modes as described above. The $\alpha_{1C}+\beta_{2a}$ channels had consistently higher Z values (see Methods) between 3·11 and 13·6 ($n = 8$), which were all above the critical value of 1·64 ($P \leq 0{\cdot}05$). Thus, in the presence of the β_{2a} subunit, the channels did not randomly switch between modes. In the α_{1C} channels we obtained lower Z values ranging between 0·31 and 8·91 ($n = 7$). In two α_{1C} experiments the Z values (0·31 and 0·42) were lower than the critical 1·64 Z value, indicating randomness. The remaining five α_{1C} experiments showed a tendency to clustering. The overall higher Z values obtained for the runs analysis in the presence of the β_{2a} subunit show a further deviation from random mode switching, which indicate that the β_{2a} subunit further stabilizes a given mode of gating.

χ^2 analysis of contingency tables (Plummer & Hess, 1991) was performed to determine whether a given gating mode during a sweep (n), was contingent on the mode of the previous sweep ($n-1$). The χ^2 values obtained from the $\alpha_{1C}+\beta_{2a}$ contingency tables were between 8·5 and 144·1 for the observed *versus* expected frequencies ($n = 4$). These values of χ^2 indicate that the $\alpha_{1C}+\beta_{2a}$ channels show a non-random pattern of clustering of sweeps. Stated differently, the mode of a given (n) sweep is non-independent of the mode during the previous ($n-1$) sweep when the β_{2a} subunit is present. The χ^2 values obtained from the α_{1C} channel had a large variability ranging between 0·002 and 101·9. In three of seven experiments, the χ^2 values indicated independence in mode switching during the time window between two consecutive sweeps. The remaining ones showed non-independence. An example of the tables obtained for two individual experiments is shown in Fig. 6. The β_{2a} subunit increased the number of high P_o sweeps followed by another high P_o sweep (Fig. 6*B*).

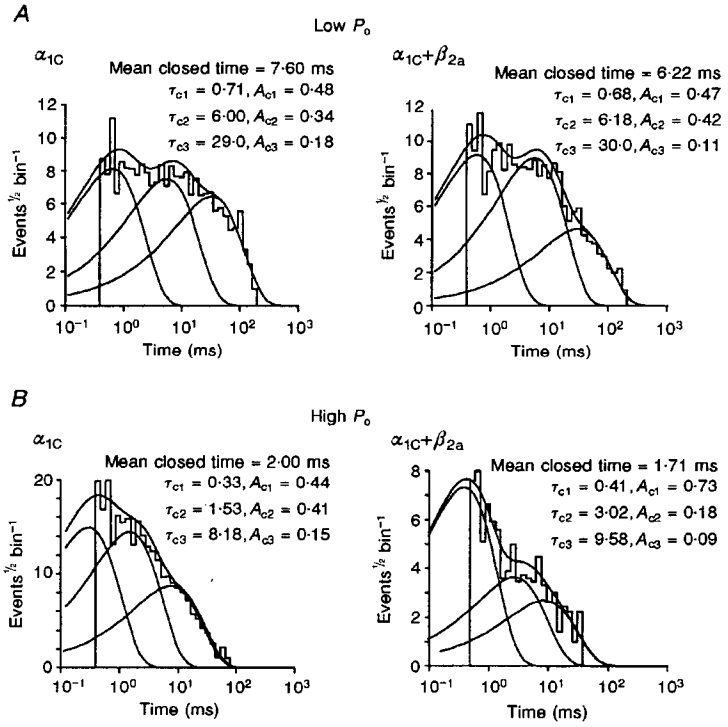

Figure 5. Closed dwell time histograms for low P_o and high P_o

Coexpression of the β_{2a} subunit increases the proportion of the briefer closed times in high P_o. Closed time histograms separated into low P_o (*A*) and high P_o (*B*), bin width is 0·07. The continuous lines are the fits to the individual peaks in each histogram and to the total histograms. Time constants (in ms) and relative amplitudes of the individual components are listed for each histogram. Bay K 8644 (10 μM) is present in the solution.

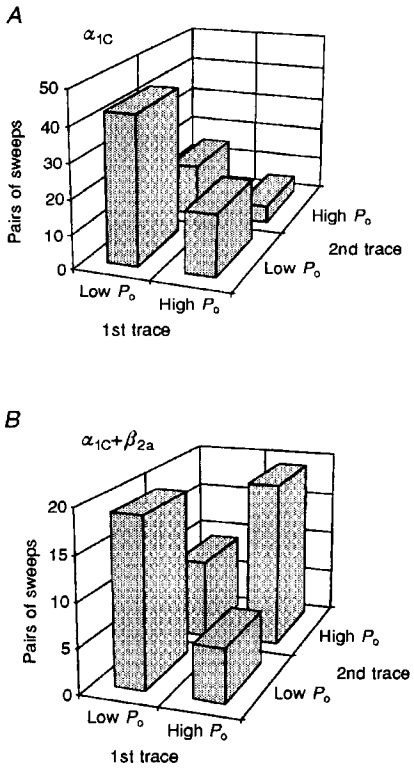

Figure 6. The β_{2a} subunit caused an increase in the clustering of sweeps in the same mode
Clustering of sweeps of the same mode is more likely to occur in the presence of the β_{2a} subunit. Contingency tables from a pair of experiments comparing low P_o and high P_o gating in the α_{1C} (*A*) and the $\alpha_{1C}+\beta_{2a}$ (*B*) channel. In the presence of the β_{2a} subunit, the mode of a sweep (n) becomes non-independent of the mode of the previous sweep ($n-1$). The (high P_o–high P_o) column is larger in *B* than in *A*, indicating clustering of consecutive high P_o sweeps in $\alpha_{1C}+\beta_{2a}$ channels, as opposed to frequent switches back and forth between the two modes in α_{1C} alone channels. The experiment analysed in *A* had a χ^2 value of 0·01, meaning that, in this case, the two characteristics that define the contingency table are not significantly related ($P = 0{\cdot}9185$). The χ^2 value for the experiment in *B* was 8·51, meaning that the two characteristics that define the contingency table are significantly related ($P = 0{\cdot}0035$). The relatively large (low P_o–low P_o) columns in both *A* and *B* are due to the fact that the majority of active traces gate in low P_o.

Taken together, the runs and contingency table analysis indicate that a non-random pattern of mode switching occurs between sweeps in the $\alpha_{1C}+\beta_{2a}$ channels. The α_{1C} channels showed some variability but a tendency of non-independence in consecutive sweeps. The β_{2a} subunit significantly increased the tendency toward clustering as seen using both methods of analysis.

DISCUSSION

A minimum model for the action of β_{2a} subunit

The effect of the β_{2a} subunit on the fast and slow gating of the α_{1C} channel can be represented by a minimal multistate model. The scheme (Fig. 7) summarizes the open, closed and inactivated states and the transitions between them. The two closed states C_{1n} and C_{2n} represent the final closed states for each mode before channel opening, the three dots represent the pathway to deeper closed states. The three open states O_{21}, O_{22}, and O_{23} represent the three open states regularly seen in high P_o open time histograms. In the absence of the β_{2a} subunit, high P_o openings are predominantly transitions from C_{2n} to O_{21} and O_{22} with less frequent transitions to O_{23}. The main effect of the β_{2a} subunit on fast C_{2n} to O transitions in high P_o is an increase in transitions from C_{2n} to O_{23} and a decrease in transitions to O_{22}. The facilitation by the β_{2a} subunit of a long open state during high P_o gating occurs through an increase in the forward rates to channel opening and not by a decrease in the backward rates away from channel opening, no new open time is created by the β_{2a} subunit and thus the backward rates leading away from the three high P_o open states are unchanged. The open state O_{11} represents the low P_o open states lumped together into one, and I_1 represents the inactivated state reached from the low P_o open states.

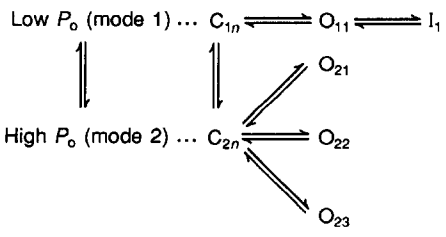

Figure 7. A multistate model for the effect of the β_{2a} subunit on α_{1C} single channel gating
A scheme depicting the open (O), closed (C) and inactivated (I) states of the channel and the effect of the β_{2a} subunit on the transitions between them.

The model also describes the decrease in mode switching caused by the β_{2a} subunit. The stabilization of high P_o gating seen within individual sweeps is incorporated into the model by decreasing the vertical rates between high and low P_o. The increase in clustering of sequential sweeps caused by the β_{2a} subunit can also be represented as a decrease in the vertical rates between the different modes. There is not a change in the proportion of null, low P_o and high P_o sweeps, suggesting that the ratio of these vertical rates between channel states remains unchanged.

Single channel modal gating is a highly conserved feature of voltage gated calcium and other channels. Our results indicate that in the presence of Bay K 8644, the β_{2a} subunit confers significant changes to both fast and slow gating processes without creating any new open state. The β_{2a} subunit alters fast gating by facilitating movement of the channel into an existing open state. Additionally, the β_{2a} subunit decreases the slow switching between modes both within the time course of a single sweep, and during the interval between sweeps, effectively creating a protein that is less willing to undergo slow conformational changes between gating modes.

Bean, B. P. (1989). Neurotransmitter inhibition of neuronal calcium currents by changes in channel voltage dependence. *Nature* **340**, 153–156.

Bean, B. P. (1990). Calcium channels: gating for the physiologist. *Nature* **348**, 192–193.

Brownlee, K. A. (1965). *Statistical Theory and Methodology in Science and Engineering*. Wiley, New York.

Catterall, W. A. (1991). Functional subunit structure of voltage-gated calcium channels. *Science* **253**, 1499–1500.

Delcour, A. H. & Tsien, R. W. (1993). Altered prevalence of gating modes in neurotransmitter inhibition of N-type calcium channels. *Science* **259**, 980–984.

Hess, P., Lansman, J. B. & Tsien, R. W. (1984). Different modes of Ca channel gating behaviour favoured by dihydropyridine Ca agonists and antagonists. *Nature* **311**, 538–544.

Hofmann, F., Biel, M. & Flockerzi, V. (1994). Molecular basis for Ca^{2+} channel diversity. *Annual Review of Neuroscience* **17**, 399–418.

Lacerda, A. E., Kim, H. S., Ruth, P., Perez-Reyes, E., Flockerzi, V., Hofmann, F., Birnbaumer, L. & Brown, A. M. (1991). Normalization of current kinetics by interaction between the α_1 and β subunits of the skeletal muscle dihydropyridine-sensitive Ca^{2+} channel. *Nature* **352**, 527–530.

Lory, P., Varadi, G., Slish, D. F., Varadi, M. & Schwartz, A. (1993). Characterization of beta subunit modulation of a rabbit cardiac L-type Ca^{2+} channel alpha 1 subunit as expressed in mouse L cells. *FEBS Letters* **315**, 167–172.

McDonald, T. F., Pelzer, S., Trautwein, W. & Pelzer, D. J. (1994). Regulation and modulation of calcium channels in cardiac, skeletal, and smooth muscle cells. *Physiological Reviews* **74**, 365–507.

Moczydlowski, E. & Latorre, R. (1983). Gating kinetics of Ca^{2+}-activated K^+ channels from rat muscle incorporated into planar lipid bilayers. Evidence for two voltage-dependent Ca^{2+} binding reactions. *Journal of General Physiology* **82**, 511–542.

Neely, A., Wei, X., Olcese, R., Birnbaumer, L. & Stefani, E. (1993). Potentiation by the β subunit of the ratio of the ionic current to the charge movement in the cardiac calcium channel. *Science* **262**, 575–578.

Olcese, R., Qin, N., Schneider, T., Neely, A., Wei, X., Stefani, E. & Birnbaumer, L. (1994). The amino terminus of a calcium channel β subunit sets rates of channel inactivation independently of the subunit's effect on activation. *Neuron* **13**, 1433–1438.

Perez-Garcia, M. T., Kamp, T. J. & Marban, E. (1995). Functional properties of cardiac L-type calcium channels transiently expressed in HEK293 cells. Role of α_1 and β subunits. *Journal of General Physiology* **105**, 289–306.

Perez-Reyes, E., Castellano, A., Kim, H. S., Bertrand, P., Baggstrom, E., Lacerda, A. E., Wei, X., Birnbaumer, L. & Wei, X. Y. (1992). Cloning and expression of cardiac/brain β subunit of the L-type calcium channel. *Journal of Biological Chemistry* **267**, 1792–1797.

Perez-Reyes, E., Kim, H. S., Lacerda, A. E., Horne, W., Wei, X., Rampe, D., Campbell, K. P., Brown, A. M. & Birnbaumer, L. (1989). Induction of calcium currents by the expression of the α_1-subunit of the dihydropyridine receptor from skeletal muscle. *Nature* **340**, 233–236.

Pietrobon, D. & Hess, P. (1990). Novel mechanism of voltage-dependent gating in L-type calcium channels. *Nature* **346**, 651–655.

Plummer, M. R. & Hess, P. (1991). Reversible uncoupling of inactivation in N-type calcium channels. *Nature* **351**, 657–659.

Reuter, H., Stevens, C. F., Tsien, R. W. & Yellen, G. (1982). Properties of single calcium channels in cardiac cell culture. *Nature* **297**, 501–504.

Rittenhouse, A. R. & Hess, P. (1994). Microscopic heterogeneity in unitary N-type calcium currents in rat sympathetic neurons. *Journal of Physiology* **474**, 87–99.

Sigworth, F. J. & Sine, S. M. (1987). Data transformations from improved display and fitting of single channel dwell time histograms. *Biophysical Journal* **52**, 1047–1054.

Singer, D., Biel, M., Lotan, I., Flockerzi, V., Hofmann, F. & Dascal, N. (1991). The roles of the subunits in the function of the calcium channel. *Science* **253**, 1553–1557.

VanDongen, A. M. (1996). A new algorithm for idealizing single ion channel data containing multiple unknown conductance levels. *Biophysical Journal* **70**, 1303–1315.

Varadi, G., Lory, P., Schultz, D., Varadi, M. & Schwartz, A. (1991). Acceleration of activation and inactivation by the beta subunit of the skeletal muscle calcium channel. *Nature* **352**, 159–162.

Wei, X. Y., Perez-Reyes, E., Lacerda, A. E., Schuster, G., Brown, A. M. & Birnbaumer, L. (1991). Heterologous regulation of the cardiac Ca^{2+} channel alpha 1 subunit by skeletal muscle beta and gamma subunits. Implications for the structure of cardiac L-type Ca^{2+} channels. *Journal of Biological Chemistry* **266**, 21943–21947.

Williams, M. E., Feldman, D. H., McCue, A. F., Brenner, R., Velicelebi, G., Ellis, S. B. & Harpold, M. M. (1992). Structure and functional expression of alpha 1, alpha 2, and beta subunits of a novel human neuronal calcium channel subtype. *Neuron* **8**, 71–84.

ZAR, J. H. (1974). *Biostatistical Analysis.* Prentice–Hall, Englewood Cliffs, NJ, USA.

Acknowledgements

This work was supported by NIH grants AR38970 to E.S. and AR43411 to L.B. N.Q. is the recipient of the AHA Scientist Development Grant 9630053N.

Corresponding author

E. Stefani: UCLA School of Medicine, Department of Anesthesiology, BH-612 CHS, Box 951778, Los Angeles, CA 90095-1778, USA.

Email: estefani@ucla.edu

Author's present address

J. Costantin: Department of Neurology, UCLA School of Medicine, UCLA, Los Angeles, CA 90024, USA.

Email: jcostant@ucla.edu